Cross sections and electromagnetic response functions for radiative proton capture in pd -> He-3+e(+)e(-)

Messchendorp, JG; Bacelar, JCS; van Goethem, MJ; Harakeh, MN; Hoefman, M; Huisman, H; Kalantar-Nayestanaki, N; Korchin, AY; Lohner, H; Ostendorf, RW

Published in:
Physics Letters B

DOI:
10.1016/S0370-2693(00)00441-X

Publication date:
2000

25 May 2000

PHYSICS LETTERS B

ELSEVIER

Physics Letters B 481 (2000) 171–176

Cross sections and electromagnetic response functions for radiative proton capture in $pd \to {}^3\mathrm{He} + e^+e^-$

J.G. Messchendorp [a,1], J.C.S. Bacelar [a], M.J. van Goethem [a], M.N. Harakeh [a], M. Hoefman [a], H. Huisman [a], N. Kalantar-Nayestanaki [a], A.Yu. Korchin [a,2], H. Löhner [a], R.W. Ostendorf [a], S. Schadmand [a,1], O. Scholten [a], M. Volkerts [a], H.W. Wilschut [a], R.S. Simon [b]

[a] *Kernfysisch Versneller Instituut, Zernikelaan 25, 9747 AA Groningen, The Netherlands*
[b] *Gesellschaft für Schwerionenforschung, Planckstraße 1, D-64291 Darmstadt, Germany*

Received 21 January 2000; accepted 31 March 2000
Editor: V. Metag

Abstract

Exclusive differential cross sections of virtual-photon radiative proton capture in $pd \to {}^3\mathrm{He} + e^+e^-$ at a proton energy of 190 MeV have been measured for the first time. The leptonic-angle dependence of the measured cross section is exploited in order to determine the electromagnetic response functions in the time-like region. The data are compared to a relativistic gauge-invariant impulse approximation and a Faddeev calculation. Differences between theoretical predictions and data are discussed in terms of enhanced magnetic radiation possibly originating from virtual Δ excitations.

PACS: 13.75.Cs; 25.10.+s; 25.20.Lj

Radiative capture and its time-reversed process, photodisintegration, are well known as a valuable source of information on the high-momentum components of the nuclear wave function. Due to the large momentum mismatch, these reactions are correspondingly sensitive to two- and three-body mechanisms. In this respect, the study of the radiative capture into ^{3}He is particularly important. This three-body system forms the bridge between the simple two-body nucleon-nucleon case and heavier nuclei.

While the real-photon radiative capture $pd \to {}^3\mathrm{He} + \gamma$ has been extensively studied for proton energies between 100 and 500 MeV [1–7], information on the corresponding virtual-photon process $pd \to {}^3\mathrm{He} + e^+e^-$ is scarce. The only measurements available [7] are for proton energies of 98 and 176 MeV. Furthermore, the data are confined to two photon angles (40° and 80°) and to virtual-photon masses smaller than 8 MeV. The virtual-photon process is particularly interesting since the dependence on the polar

[1] Present address: Universität Gießen, Heinrich-Buff-Ring 16, D-35392 Gießen, Germany.
[2] Permanent address: NSC, Kharkov Institute of Physics and Technology, 310108 Kharkov, Ukraine.

0370-2693/00/$ - see front matter
PII: S0370-2693(00)00441-X

and azimuthal angles of the observed lepton pair determines photon-polarization observables which are conventionally cast in the form of Response Functions (RFs). In addition, the virtual photon can be longitudinally polarized. Polarization observables are important to understand the dynamics of the process. In particular, Ref. [8] showed that for virtual-photon emission from proton-proton collisions, the transverse RFs are particularly sensitive to non-nucleonic degrees of freedom whereas the longitudinal RFs are influenced by the inclusion of negative-energy states.

In this Letter, we present the first measurement of the cross section for $p + d$ virtual-photon capture just below pion-production threshold, an energy regime which is specially suited to probe mesonic degrees of freedom and hadronic excitations in nuclei. The beam energy of 190 MeV ($E^{\mathrm{CM}} = 130$ MeV) and the photon angular range covered (60° to 170°) are of particular interest since a large discrepancy between microscopic model predictions and the real-photon radiative-capture cross sections (measured concurrently in the present experiment) is known to exist [1,3,5,9]. Exploiting the wide range covered for the observables of the virtual photon, we demonstrate for the first time the possibility to extract the electromagnetic RFs from the measured differential cross sections. A cylindrical liquid-deuterium target (20 mm diameter and 126 mg/cm^2 thick [10]), with 4 μm thin aramid windows, was used. The Small-Angle Large-Acceptance Detector, SALAD [11], allowed to measure the direction of the outgoing ^{3}He for polar angles $> 6°$ and full azimuthal coverage. The Two-Arm Photon Spectrometer, TAPS [12], was used to measure the momentum of the real photon or the directions and energies of the two leptons following virtual-photon radiative capture. In the latter case the thin plastic scintillators in front of the BaF_2 crystals of TAPS were used to identify the leptons. Polar angles between 60° and 170° were covered in a broad azimuthal band on either side of the beam. Detector efficiencies and other details of the setup can be found elsewhere [13,14].

With the momenta and kinetic energy of all three outgoing particles measured (in total 9 observables), the kinematics of the reaction is overdetermined since only 5 observables are independent (the other four are constrained by momentum and energy conservation). From any five measured observables one can calculate the remaining four observables for that event and compare them with the measured values. Setting windows on this comparison eliminates background (random) events. Furthermore, time of flight information has been exploited to reduce the experimental background to a negligible level. This is extensively discussed in a forth coming paper [13]. In Fig. 1 a well-defined capture peak can be observed for both the real- and virtual-photon cases, with no evidence for background contamination. The lower centroid energy in the virtual-photon spectrum is due to the energy loss of the leptons traversing the thin plastic scintillators and their light-guides. The known response of TAPS reproduces the experimental energy distribution, demonstrating that the background is indeed negligible.

Using the integrated beam intensity obtained by a Faraday cup, differential cross sections as a function of $\theta_\gamma^{\mathrm{CM}}$ and for virtual radiative capture also as function of M_γ have been determined. For the experimental determination of differential cross sections,

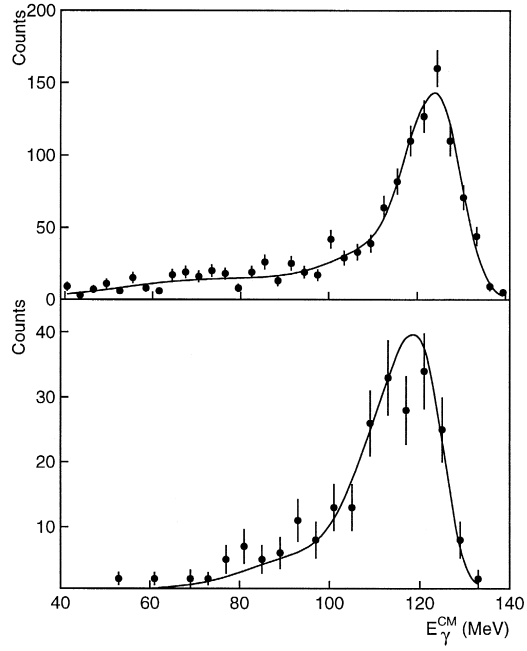

Fig. 1. Photon CM energy spectra for the $pd \to {}^3\mathrm{He} + \gamma^{(*)}$ process at a bombarding energy of 190 MeV as measured with TAPS for real (top) and virtual (bottom) photons. The solid lines represent the simulated response of TAPS.

the data were corrected for the calculated acceptances and the measured detector efficiencies [13,14]. The total systematic uncertainty of $\pm 17\%$ is due to the uncertainty in the integrated luminosity of 370 ± 40 pb^{-1}, and in the detector efficiencies. We have identified 12000 real-photon capture events and 300 events from the $pd \to {}^3\mathrm{He} + e^+e^-$ reaction. Only events with invariant mass $M_\gamma > 15$ MeV were selected [13,14].

The differential cross section as a function of $\theta_\gamma^{\mathrm{CM}}$ is shown in Fig. 2, for both real- (top panel) and virtual-photon (bottom panel) capture processes. The real-photon capture cross sections are in good agreement with previously published data [5–7]. Furthermore, the data are compared to calculations with a relativistic gauge-invariant model [3] (dotted curve) and a recent Faddeev calculation [15] (dashed curve). The latter includes initial-state interactions as well as π and ρ meson exchange currents explicitly, with the method outlined in Ref. [16]. The calculation shown as the dotted curve is qualitatively in agreement with the microscopic calculations of Laget [1], where the one- and two-pion exchange contributions are explicitly calculated. The solid line is discussed below.

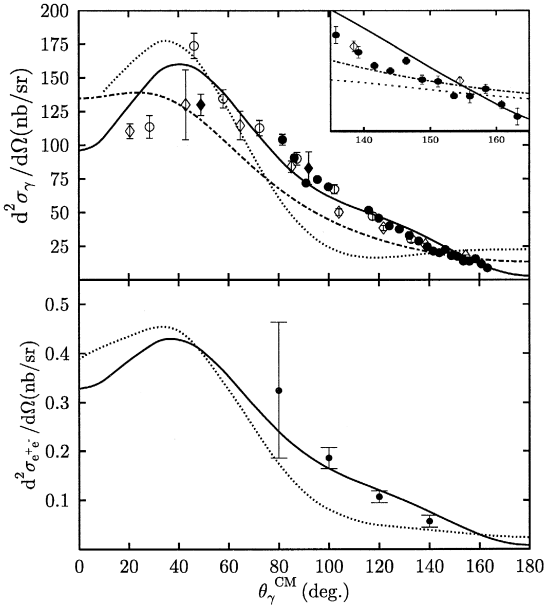

Fig. 2. The real- (top) and virtual-photon (bottom) capture cross sections of the $pd \to {}^3\mathrm{He} + \gamma^{(*)}$ reaction as a function of $\theta_\gamma^{\mathrm{CM}}$. Present data are shown as full dots. Empty dots, and full and empty diamonds are data from Refs. [5–7], respectively. The lines are the results of calculations using a relativistic gauge-invariant model (solid and dotted curves) and a Faddeev calculation (dashed curve) as discussed in the text. For the virtual-photon case the data and calculations are integrated for $M_\gamma > 15$ MeV.

The experimental differential cross section for the virtual-photon capture process is compared with the same relativistic gauge-invariant model as used for the real photon case but extended to include virtual photons [3], dotted lines in Figs. 2, 4 and 5. In this model, the amplitude includes radiation from all external particles. Other contributions, such as meson-exchange diagrams, are not explicitly calculated but are effectively included via an internal (or contact) amplitude constructed by applying gauge invariance. The covariant $\langle {}^3\mathrm{He}|\, pd\rangle$ vertex is based on a calculation of ^{3}He [17] with the recent Argonne v18 nucleon-nucleon potential together with the Urbana IX three-nucleon interaction. The discrepancy noted for the real-photon capture cross section is also observed for the virtual-photon capture process in the angular range $70° < \theta_\gamma^{\mathrm{CM}} < 140°$. The experimental ratio of the real-photon cross section to the virtual-photon cross section (integrated for $M_\gamma > 15$ MeV) is $(2.5 \pm 0.2) \times 10^{-3}$, in agreement with the theoretical prediction of 2.6×10^{-3} [3,13].

The differential cross section, in the CM frame, for the $pd \to {}^3\mathrm{He} + e^+e^-$ process can be decomposed into longitudinal, transverse, transverse-transverse and longitudinal-transverse components [2,3]:

$$\begin{aligned}\frac{d^5\sigma_{e^+e^-}}{d\Omega_\gamma\, dM_\gamma\, d\Omega_\ell} = {} & \frac{\alpha^2 P_{e^+e^-} m_p m_{\mathrm{He}}}{8\pi^3 s}\,\frac{|\boldsymbol{k}|}{|\boldsymbol{p}|}\,\frac{1}{M_\gamma} \\ & \times \left\{ \left(1 - \frac{2\boldsymbol{l}^2}{M_\gamma^2}\sin^2\theta_\ell\right) W_T \right. \\ & + \left(1 - \frac{4\boldsymbol{l}^2}{k_0^2}\cos^2\theta_\ell\right) W_L \\ & + \frac{2\boldsymbol{l}^2 \sin^2\theta_\ell}{M_\gamma^2} W_{TT} \cos 2\phi_\ell \\ & \left. + \sqrt{2}\,\frac{\boldsymbol{l}^2 \sin 2\theta_\ell}{k_0 M_\gamma} W_{LT} \cos\phi_\ell \right\}, \end{aligned} \tag{1}$$

with α the fine-structure constant, $|\boldsymbol{k}|$ and $|\boldsymbol{p}|$ the absolute momenta of the virtual photon (mass M_γ)

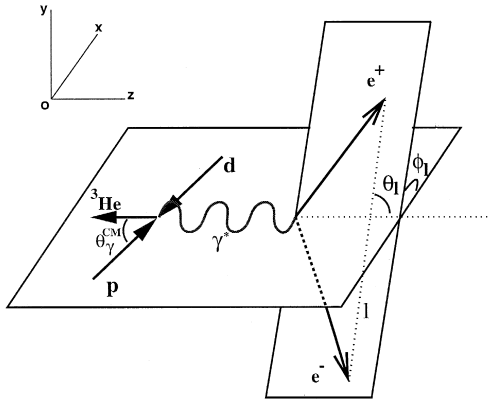

Fig. 3. Schematic diagram, in the CM frame, for the reaction $pd \to {}^3\mathrm{He} + e^+ e^-$. Shown are the polar angle, $\theta_\gamma^{\mathrm{CM}}$, and the two leptonic angles θ_ℓ, ϕ_ℓ corresponding to the polar and azimuthal angles of the momentum-vector $\boldsymbol{l} = \frac{1}{2}(\boldsymbol{k}_+ - \boldsymbol{k}_-)$.

and of the incoming proton (mass m_p), respectively, and k_0 the photon energy; m_{He} is the mass of the ^{3}He and s the invariant energy squared. The variables describing the leptons $\boldsymbol{l}$, θ_ℓ and ϕ_ℓ are shown in Fig. 3, the factor $P_{e^+e^-} = 4|\boldsymbol{l}|^3/k_0(M_\gamma^2 - 4m_e^2)$ comes from the evaluation of the leptonic phase-space in the CM frame, where m_e is the electron mass. $k = k_+ + k_-$ is the 4-momentum of the virtual photon and (k_+, k_-) are the 4-momenta of the e^+ and e^-, respectively. The electromagnetic RFs, W_i, depend on s, M_γ and $\theta_\gamma^{\mathrm{CM}}$ [3,9]. At small invariant masses W_T is similar to the quantity measured in an unpolarized real-photon capture; it is an incoherent sum of the photon helicity $\lambda_{\gamma^*} = +1$ and $\lambda_{\gamma^*} = -1$ contributions. The interference of these two amplitudes is expressed in W_{TT}, and at small invariant masses it is equivalent to asymmetry measurements with linear-polarized photons in the reaction $\gamma + {}^3\mathrm{He} \to pd$. Finally, W_L and W_{LT} are specific for dilepton production and in particular W_L carries information on the radial current distribution.

To extract the RFs from the data we follow the procedure described in [13,14]. For the transverse RF averaged over the experimentally-covered $\theta_\gamma^{\mathrm{CM}}$, events for which the energy-sharing angle $\theta_\ell < 40^\circ$ are selected in order to minimize the contribution from W_L (see Eq. (1)). For these events the integrated cross section as a function of M_γ is determined and divided by the phase-space integral (obtained from a Monte Carlo integration). The result of this analysis is shown in Fig. 4. Over the entire $\theta_\gamma^{\mathrm{CM}}$ angle covered by this experiment the model (dotted line) underestimates $\overline{W}_T$. To extract all other RFs, the non-vanishing contribution of W_T has to be subtracted from the data. This is done with the help of a model which can fit well the measured cross sections. Refs. [13,14] have shown that the extracted RFs are then only weakly dependent on the model predictions for W_T. In an attempt at fitting the real-photon cross sections, Ref. [9] introduces an ad-hoc parameter (α) which enhances the magnetic contribution. Calculations of this model with $\alpha = 1.2$ are shown as solid lines in Figs. 2, 4 and 5. This value of α is chosen such that it best fits the real-photon capture cross sections at 190 MeV. With the prediction of this model for W_T (solid line in Fig. 4) the other RFs are extracted from the data. The error bars shown in Figs. 4 and 5, include the statistical accuracy of the data as well as the systematic error associated with the uncertainty in fitting the transverse response function to the measured data. Analysing the events with $\theta_\ell > 40^\circ$ (to enhance the longitudinal contribution) the data show that the extracted longitudinal RF is consistent with zero for all photon masses, which is consistent with the small values predicted by theory.

To study the interference RFs W_{TT} and W_{LT}, the $\cos 2\phi_\ell$ and $\cos\phi_\ell$ dependence of the cross section (see Eq. (1)) is exploited. Furthermore, we have divided the data-set into two regions of the polar angle of the virtual photon $70^\circ < \theta_\gamma^{\mathrm{CM}} < 105^\circ$ and $120^\circ < \theta_\gamma^{\mathrm{CM}} < 145^\circ$, respectively. In Fig. 5, the ex-

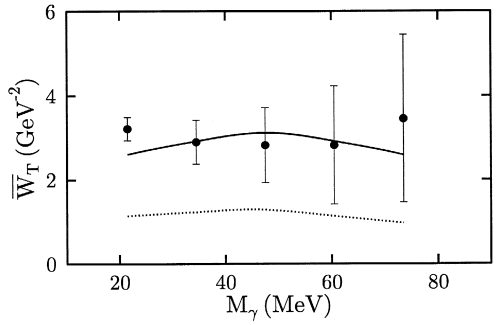

Fig. 4. The averaged transverse RF, $\overline{W}_T$, as a function of the invariant mass, M_γ, for energy-sharing angles of $\theta_\ell < 40^\circ$. The data are shown as solid dots, with a bin width of 13 MeV. The solid and dotted lines are the results of the calculations performed with a relativistic gauge-invariant model as discussed in the text.

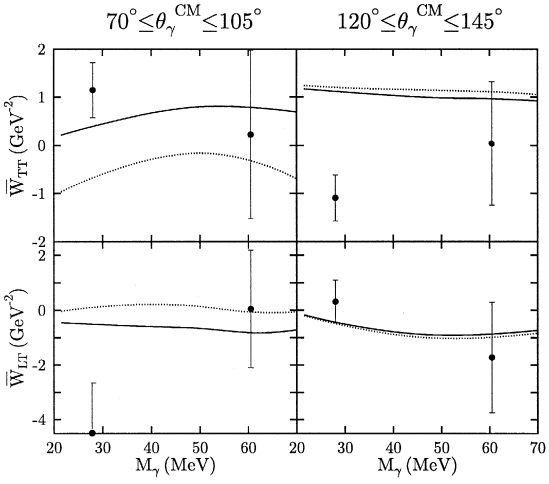

Fig. 5. The averaged RFs $\overline{W}_{TT}$ (top panel) and $\overline{W}_{LT}$ (bottom panel) as a function of the photon mass M_γ for two ranges in the polar angle of the virtual photon. The bin size of the data is 25 and 40 MeV for the low- and high-M_γ data points, respectively. The solid and dotted lines are the results of calculations performed with a relativistic gauge-invariant model as discussed in the text.

tracted averaged RFs $\overline{W}_{TT}$ (top panel) and $\overline{W}_{LT}$ (bottom panel) are shown.

For small M_γ ($15 < M_\gamma < 40$ MeV), the data indicate a sign change of $\overline{W}_{TT}$ in going from virtual-photon polar angles $70° < \theta_\gamma^{\rm CM} < 105°$ towards backward angles $120° < \theta_\gamma^{\rm CM} < 145°$. The calculation (dotted lines on the top panel of Fig. 5) does predict a sign change but with the opposite phase. For $\overline{W}_{LT}$, the data are described by the calculation, except for small M_γ in the region $70° < \theta_\gamma^{\rm CM} < 105°$. Furthermore, our analysis confirms that contributions to the RFs that are proportional to $\sin\phi_\ell$ and $\sin 2\phi_\ell$ are absent, as required for a reaction with a two-body final state [2,3,9]. In general for a three-body final state these RFs are non-zero. This fact was experimentally verified for the $pp \to pp + e^+e^-$ reaction [14]. The large discrepancy between theoretical predictions and experimental data for both the real- and virtual-photon capture cross sections implies enhanced transverse radiation which could be attributed to magnetic contributions. An example of such a process is the virtual excitation of the Δ. This process is not taken into account in the theoretical predictions shown as dotted lines in Figs. 2, 4 and 5, and also not in the Faddeev calculations [15] (dashed line in Fig. 2), nor in the calculations of Laget [1].

It is interesting to note that the ad-hoc modification introduced into the impulse approximation model to fit the cross section, affects the RFs in different ways (cf. solid and dotted curves in Figs. 4 and 5), demonstrating the model sensitivity of the RFs.

In summary, for the real- and virtual-photon processes, $pd \to {}^3\mathrm{He} + \gamma^{(*)}$, differential cross sections as a function of the polar angle of the photon in the CM frame are obtained. For the virtual-photon capture process, we have for the first time studied the decomposition of the $pd \to {}^3\mathrm{He} + e^+e^-$ cross section into four electromagnetic RFs. Large discrepancies are observed between calculations and data. This could be interpreted as enhanced magnetic radiation in the capture process, pointing to the importance of processes such as virtual Δ excitation. Microscopic calculations [8] have shown that contributions from virtual Δ excitation are important in proton-proton bremsstrahlung at similar CM energies. Future planned experiments aim at determining the RFs with higher accuracy since, as shown here, these observables provide unique sensitivity to theoretical models.

Acknowledgements

The authors acknowledge the support by the TAPS collaboration and thank L. Dieperink, R. Timmermans, and J. Tjon for valuable discussions and J. Golak for providing the Faddeev results. This work is part of the research program of the ''Stichting voor Fundamenteel Onderzoek der Materie'' (FOM) with financial support from the ''Nederlandse Organisatie voor Wetenschappelijk Onderzoek'' (NWO) and by the European Union HCM network under Contract No. HRXCT94066.

References

[1] J.M. Laget, Phys. Rev. C 38 (1988) 2993.
[2] D. Van Neck et al., Nucl. Phys. A 574 (1994) 643.
[3] A.Yu. Korchin et al., Phys. Lett. B 441 (1998) 17.
[4] J.P. Didelez et al., Nucl. Phys. A 143 (1970) 602.
[5] J.M. Cameron et al., Nucl. Phys. A 424 (1984) 549.
[6] M.J. Pickar et al., Phys. Rev. C 35 (1987) 37.
[7] R. Johansson et al., Nucl. Phys. A 641 (1998) 389.
[8] G. Martinus et al., Few-Body Syst. 26 (1999) 197.

[9] A.Yu. Korchin et al., Phys. Rev. C 59 (1999) 1890.
[10] N. Kalantar-Nayestanaki, J. Mulder, J. Zijlstra, Nucl. Instr. and Meth. Phys. Res. A 417 (1998) 215.
[11] N. Kalantar-Nayestanaki et al., Nucl. Instr. Meth. Phys. Res, in press.
[12] A.R. Gabler et al., Nucl. Instr. Meth. Phys. Res. A 346 (1994) 168.
[13] J.G. Messchendorp, Ph.D. thesis, University of Groningen (1999); Phys. Rev. C submitted.
[14] J.G. Messchendorp et al., Phys. Rev. Lett. 82 (1999) 2649; Phys. Rev. Lett. 83 (1999) 2530.
[15] J. Golak, private communication; W. Glöckle et al., Phys. Rep. 274 (1996) 107.
[16] R. Schiavilla et al., Phys. Rev. C 40 (1989) 2294.
[17] J.L. Forest et al., Phys. Rev. C 54 (1996) 646; R.B. Wiringa et al., Phys. Rev. C 51 (1995) 38.